







Table 1. Cross Reactivity (%) of Nanopeptamer pA and PHAIA Assays with Related Thiocarbamate Pesticides<sup>a</sup>

<sup>a</sup>All data are the mean of two independent experiments. A value of 0 means that there was no observable cross-reactivity at the highest concentration tested, 10<sup>4</sup> ng/mL.

molinate curves were performed with undiluted agricultural runoff-water samples from different areas of Uruguay (Figure S-4, Supporting Information).

**Nanopeptamers Allow the Development of Non-competitive Lateral-Flow Tests.** A major advantage of noncompetitive assays is that they can be developed into simple formats with a positive visual end point. Our initial attempts to adapt PHAIA into lateral-flow assays were not successful, most probably due to the filamentous nature of the phage that promoted the formation of aggregates with the colloidal labels. Fortunately, this limitation was overcome using nanopeptamers. Figure 3A shows the results of a lateral-flow assay set up using MoAb 14D7 as the capture reagent immobilized on

polyester-backed nitrocellulose membranes and colloidal-carbon labeled avidin complexed to pA for detection (see the Supporting Information). For the sake of comparison, we also developed the molinate assay in a lateral-flow competitive format using MoAb 14D7 as capture antibody and the molinate derivative 7b (S-2-(*p*-aminophenyl)-ethyl-hexahydroazepine-1-carbothioate) coupled to conalbumin, which was labeled with colloidal carbon for detection, Figure 3B. A molinate concentration of 2.5 ng/mL caused a visible test line in the noncompetitive assay, while 32 ng/mL produce a weaker test line than the negative control in the competitive assay, as was agreed upon by four independent observers in three different repetitions of the test. This is in agreement with the densitometry analysis of the strips, Supporting Table S-1A (Supporting Information). In addition to the positive reading, the noncompetitive test performed with a 10-fold improved sensitivity. The assay was then tested for matrix interference using 10 runoff water samples from agricultural areas of Uruguay spiked with 0, 1.0, 1.5, 2.5, 5, and 20 ng/mL of molinate. The strips were read by four independent observers, all of whom detected a visible reaction line with concentrations of 2.5 ng/mL or higher, Figure S-5 (Supporting Information).

**Nanopeptamer Based ELISA and Lateral-Flow Test for Clomazone.** To explore the general utility of the method, we also developed nanopeptamer-based assays for the herbicide clomazone. To this end we used the anticlomazone MoAb 5.6<sup>17</sup> and the anti-IC synthetic peptide X11 (biotin-SGSGCLEAP-NIEGC) complexed with SPO or avidin. This peptide has been

**Figure 3.** Noncompetitive nanopeptamer pA-based (A) and competitive (B) lateral-flow assays for molinate. The nitrocellulose strips were tested with buffer containing various concentrations of molinate (ng/mL) as denoted in the figure.

previously isolated from phage libraries panned against the clomazone-MoAb 5.6 IC.<sup>9</sup> For ELISA, the assay conditions were optimized essentially as described for the molinate test, which allowed one to obtain a LOD = 1.2 ng/mL and SC50 = 3.4 ± 0.2 ng/mL using SPO-pX11 (Figure 4A). This represents

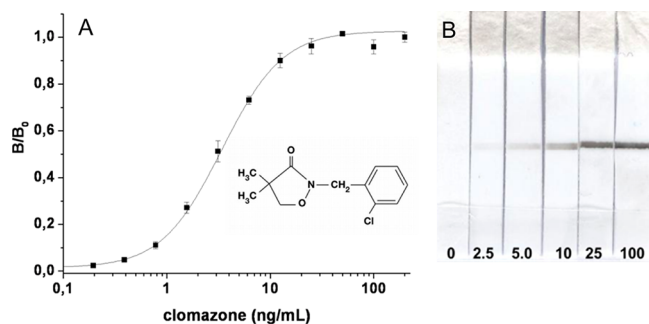


**Figure 4.** Noncompetitive nanopeptamer ELISA and lateral-flow test for clomazone using peptide pX11. (A) MoAb 5.6 (10 μg/mL) was used for coating and SPO (0.75 μg/mL) complexed with a 50-fold molar peptide excess for detection. (B) Nitrocellulose strips were tested with buffer containing various concentrations of clomazone (ng/mL) as denoted in the lower part of the figure.

an improvement of 3.3 and 8.3-fold regarding the assay setup with the same antibody in a competitive format (LOD = 4 ng/mL and IC50 = 28 ± 1.1 ng/mL, respectively).<sup>17</sup> The assay was also adapted into a lateral-flow format using avidin-pX11 labeled with carbon black, which allowed one to detect up to 2.5 ng/mL of clomazone (Figure 4B); the densitometry data is shown in Supporting Table S-1B in the Supporting Information.

## CONCLUSIONS

Our results show that in spite of big structural differences, the streptavidin/avidin-based nanopeptamer properly reproduces the binding characteristics of the phage particles. Indeed, the dihedral D2 molecular symmetry of the streptavidin homotetramer positions two pairs of biotin binding sites on opposite faces of the protein, and thus the distance between the biotin carboxylated oxygens that anchor the peptides are ~2 nm on the same face and ~3 nm on opposite faces of the complex.<sup>18</sup> On the other hand, M13 has a ~6 nm × 1000 nm rodlike structure, covered by ~2700 copies of the minor protein pVIII arranged in a fish-scale pattern, and the use of a phagemid system for the generation of the virions yields phage particles with approximately 200 copies of pVIII expressing the peptide, meaning an average distance between peptides close to 10 nm.<sup>19</sup> In addition, the peptide is tethered in a different way in both systems. For the sake of simplicity, the peptides were synthesized with a biotin residue added to their N-terminus, while they are expressed as pVIII N-terminal fusions on the phage. Considering the differences in valences and display features of both systems, it seems that the specific recognition of the IC by the peptide can be transferred out of the “phage context” with a considerable degree of flexibility.

As demonstrated here, the availability of phage-free reagents for noncompetitive assays could have a major impact in the development of rapid two-site tests for small molecules with a positive visual end point, a feat not possible with the available technology. Since the strategy for the selection of anti-IC phage borne peptides is well established, and considering the varied offer of commercially available streptavidin conjugates, nano-

peptamers may be the long-sought detection reagent for the development of fast noncompetitive assays for small analytes. In that sense a major proof of concept contributed by our work is their use in the development of lateral flow test for small molecules with a positive reading improving the sensitivity and interpretability of these tests.

## ASSOCIATED CONTENT

### Supporting Information

Additional information as noted in text. This material is available free of charge via the Internet at <http://pubs.acs.org>.

## AUTHOR INFORMATION

### Corresponding Author

\*E-mail: [ggonzal@fq.edu.uy](mailto:ggonzal@fq.edu.uy). Phone: +(598) 2487 4334.

### Author Contributions

L.V. and A.G.-T. contributed equally to this work. The manuscript was written through contributions of all authors. All authors have given approval to the final version of the manuscript.

### Notes

The authors declare no competing financial interest.

## ACKNOWLEDGMENTS

This work was supported with funds provided by grants FMV 3138 ANII (Agencia Nacional de Investigación e Innovación, Uruguay) and TW05718 Fogarty Center NHI. The support of grants P42 ES04699 and U54 OH007550 is also acknowledged. We are in debt to Patricia Noguera, Department of Chemistry, Polytechnic University of Valencia, for her help with the initial lateral-flow experiments with phage.

## REFERENCES

- (1) Hage, D. S. *Anal. Chem.* **1995**, *67*, 455R.
- (2) Ng, A. H.; Uddayasankar, U.; Wheeler, A. R. *Anal. Bioanal. Chem.* **2010**, *397*, 991.
- (3) Schneider, R. J. *Anal. Bioanal. Chem.* **2003**, *375*, 44.
- (4) Jackson, T. M.; Ekins, R. P. *J. Immunol. Methods* **1986**, *87*, 13.
- (5) Piran, U.; Riordan, W. J.; Livshin, L. A. *Clin. Chem.* **1995**, *41*, 986.
- (6) Pradelles, P.; Grassi, J.; Creminon, C.; Boutten, B.; Mamas, S. *Anal. Chem.* **1994**, *66*, 16.
- (7) Ueda, H. *J. Biosci. Bioeng.* **2002**, *94*, 614.
- (8) Gonzalez-Techera, A.; Vanrell, L.; Last, J. A.; Hammock, B. D.; Gonzalez-Sapienza, G. *Anal. Chem.* **2007**, *79*, 7799.
- (9) Rossotti, M. A.; Carlomagno, M.; Gonzalez-Techera, A.; Hammock, B. D.; Last, J.; Gonzalez-Sapienza, G. *Anal. Chem.* **2010**, *82*, 8838–8843.
- (10) Kim, H. J.; Rossotti, M. A.; Ahn, K. C.; Gonzalez-Sapienza, G. G.; Gee, S. J.; Musker, R.; Hammock, B. D. *Anal. Biochem.* **2010**, *401*, 38–46.
- (11) Gonzalez-Techera, A.; Kim, H. J.; Gee, S. J.; Last, J. A.; Hammock, B. D.; Gonzalez-Sapienza, G. *Anal. Chem.* **2007**, *79*, 9191.
- (12) Inaba, J.; Nakamura, S.; Shimizu, K.; Asami, T.; Suzuki, Y. *Anal. Biochem.* **2009**, *388*, 63.
- (13) Tanaka, F.; Hu, Y.; Sutton, J.; Asawapornmongkol, L.; Fuller, R.; Olson, A. J.; Barbas, C. F., 3rd; Lerner, R. A. *Bioorg. Med. Chem.* **2008**, *16*, 5926.
- (14) Kim, H. J.; McCoy, M.; Gee, S. J.; Gonzalez-Sapienza, G. G.; Hammock, B. D. *Anal. Chem.* **2011**, *83*, 246.
- (15) Rufo, C.; Hammock, B. D.; Gee, S. J.; Last, J. A.; Gonzalez-Sapienza, G. *J. Agric. Food Chem.* **2004**, *52*, 182.
- (16) Srisa-Art, M.; Dyson, E. C.; deMello, A. J.; Edel, J. B. *Anal. Chem.* **2008**, *80*, 7063.

(17) Carlomagno, M.; Matho, C.; Cantou, G.; Sanborn, J. R.; Last, J. A.; Hammock, B. D.; Roel, A.; Gonzalez, D.; Gonzalez-Sapienza, G. J. *Agric. Food Chem.* **2010**, *58*, 4367.

(18) Hendrickson, W. A.; Pahler, A.; Smith, J. L.; Satow, Y.; Merritt, E. A.; Phizackerley, R. P. *Proc. Natl. Acad. Sci. U.S.A.* **1989**, *86*, 2190.

(19) Martens, C. L.; Cwirla, S. E.; Lee, R. Y.; Whitehorn, E.; Chen, E. Y.; Bakker, A.; Martin, E. L.; Wagstrom, C.; Gopalan, P.; Smith, C. W.; Tate, E.; Koller, K. J.; Schatz, P. J.; Dower, W. J.; Barrett, R. W. *J. Biol. Chem.* **1995**, *270*, 21129–21136.

## Supporting Information

# Nanopeptamers for the Development of Small-Analyte Lateral Flow Tests with a Positive Readout

Lucía Vanrell<sup>#</sup>, Andrés González-Techera<sup>#</sup>, † Bruce D Hammock and Gualberto González-Sapienza<sup>#</sup>

<sup>#</sup>*Cátedra de Inmunología, Facultad de Química, Instituto de Higiene, Udelar, Montevideo 11600, Uruguay.* †*Department of Entomology and UCD Cancer Center, University of California, Davis, California 95616, United States*

- **Supporting Figure S-1.....page S1**
- **Supporting Figure S-2.....page S2**
- **Supporting Figure S-3.....page S3**
- **Supporting Figure S-4.....page S4**
- **Supporting Figure S-5.....page S5**
- **Supporting Table S-1 .....page S6**

## Supporting Figures

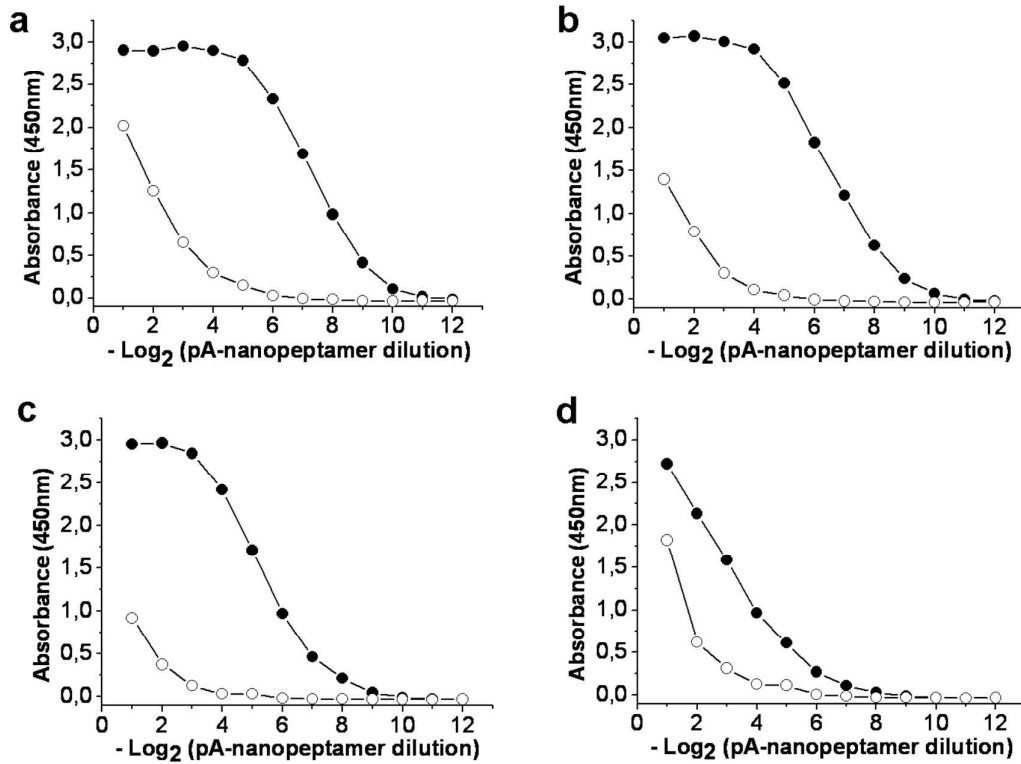


**Figure S-1. Reactivity of the pA-Nanopeptamer against the molinate-antibody immunocomplex and the uncombined antibody.** Plates were coated with 10  $\mu\text{g/mL}$  of MoAb 14D7 (a), 5  $\mu\text{g/mL}$  (b), 2.5  $\mu\text{g/mL}$  (c), or 1.25  $\mu\text{g/mL}$  (d) and incubated with two-fold serial dilutions of pA-Nanopeptamer in the presence (black circles) or absence (white circles) of molinate (100 ng/mL) using a starting concentration of Nanopeptamer concentration of 2.4  $\mu\text{g/mL}$ . An approximate 50-fold molar excess of biotinylated peptide was used for these ELISAs.



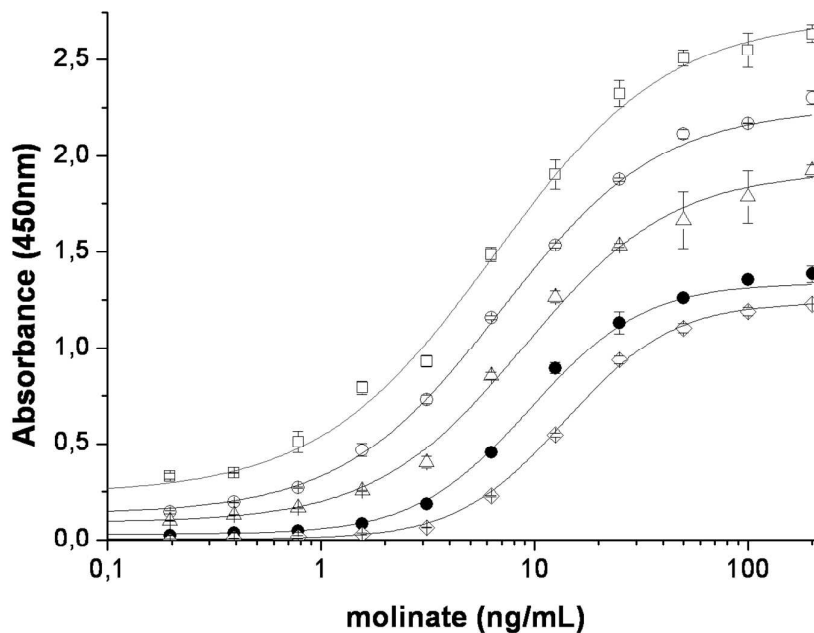


**Figure S-2. Effect of the final concentration of pA-Nanopeptamer on the molinate noncompetitive ELISA.** Microtiter plates coated with 10 µg/mL of MoAb 14D7 were incubated with two-fold serial dilutions of standard molinate and different concentrations of pA-Nanopeptamer. White squares (pA-Nanopeptamer, 6 µg/mL)  $SC_{50} = 4.0 \pm 0.3$  ng/mL; white circles (pA-Nanopeptamer, 3 µg/mL)  $SC_{50} = 3.7 \pm 0.2$  ng/mL; white triangles (pA-Nanopeptamer, 0.75 µg/mL)  $SC_{50} = 8.7 \pm 0.4$  ng/mL; black circles (pA-Nanopeptamer, 0.38 µg/mL)  $SC_{50} = 20.3 \pm 1$  ng/mL; white diamonds (pA-Nanopeptamer, 0.18 µg/mL)  $SC_{50} = 32.4 \pm 1$  ng/mL. From these experiments a final concentration of 0.75 µg/mL pA saturated SPO-pA-Nanopeptamer was chosen for further experiments.

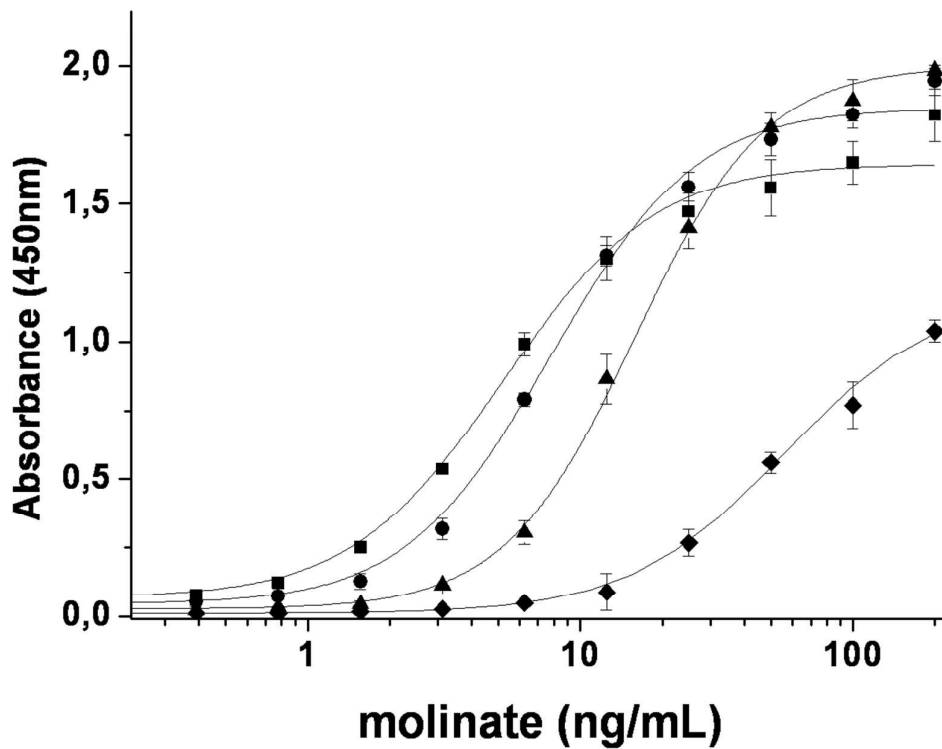


**Figure S-3. Effect of pA to SPO ratio in pA-Nanopeptamer assay performance.** Microtiter plates were coated with 10  $\mu\text{g/mL}$  of MoAb 14D7. SPO was preincubated with the approximate following molar ratios of biotinylated peptide to SPO: 50 (squares,  $SC_{50} = 5.5 \pm 0.3$ ), 6.5 (circles,  $SC_{50} = 7.7 \pm 0.3$ ), 1.5 (triangles,  $SC_{50} = 15.8 \pm 1.0$ ) and 0.6 (diamonds,  $SC_{50} = 55.6 \pm 3.42$ ). Similar results were obtained with the p1M-Nanopeptamer (not shown).

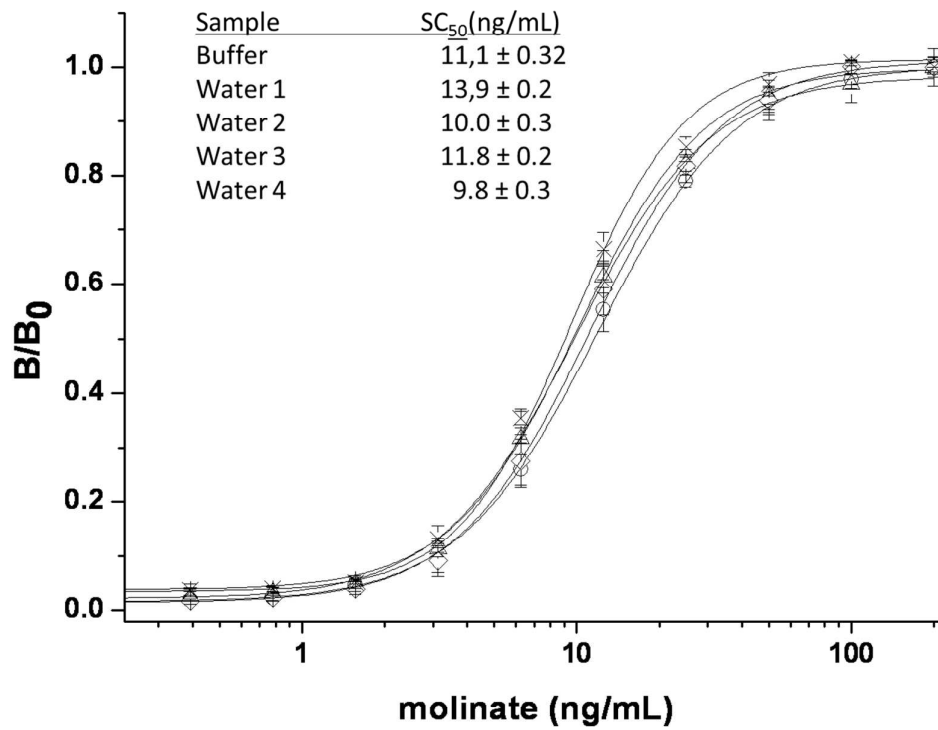


**Figure S-4. Matrix effect on the molinate pA-Nanopeptamer assay.** MoAb 14D7 (10 µg/mL) was used for coating and SPO (0.75 µg/mL) complexed with a 50 fold molar excess of pA (triangles) for detection. The test was performed with molinate dissolved in assay buffer (circles) or undiluted water from agricultural runoffs, squares, triangles, diamonds or crosses, for water samples 1-4, respectively

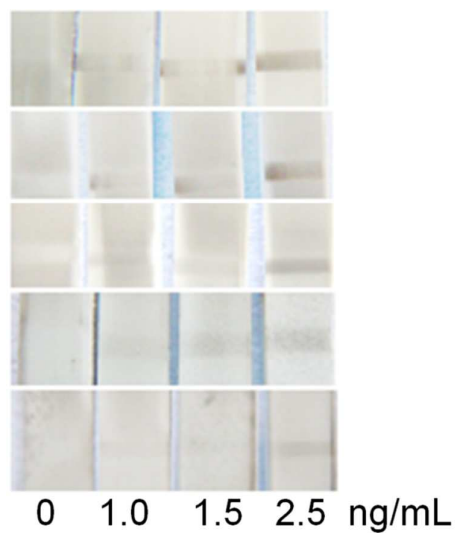


**Figure S-5. Lateral-flow analysis of molinate in surface water samples using the avidin-pA Nanopeptamer labeled with carbon-black.** Water samples from rivers and dams of Uruguay were spiked with various amounts of molinate mixed with 5% (v/v) of concentrated (10 x) PBS-T before the assay. Only the 0-2.5 ng/mL range is shown.

**Supporting Table S-1. Strip densitometry measurements of molinate and clomazone Nanopeptamers Lateral-Flow Assays. A) and B), densitometry values corresponding to lateral-flow strips shown in figures 3 and 4, respectively**

A		B	
Molinate (ng/mL)	Peak Area	Clomazone (ng/mL)	Peak Area
0	167.7	0	145.2
2.5	1087.3	2.5	565.6
5	2307.7	5	1571.3
10	3292.4	10	3875.7
25	3971.3	25	7375.3
200	8324.1	200	8058.3

Images were processed with the ImageJ software (NIH)